Differential cross section of $\gamma n \to K^+\Sigma^-$ on bound neutrons with incident photons from 1.1 to 3.6 GeV

S. Anefalos Pereira,[1] M. Mirazita,[1] P. Rossi,[1] E. De Sanctis,[1] G. Niculescu,[2] I. Niculescu,[2] S. Stepanyan,[3] K.P. Adhikari,[29] M. Aghasyan,[1] M. Anghinolfi,[20] H. Baghdasaryan,[38,29] J. Ball,[11] M. Battaglieri,[20] B.L. Berman,[18] A.S. Biselli,[15,9] C. Bookwalter,[17] D. Branford,[14] W.J. Briscoe,[18] W.K. Brooks,[36,3] V.D. Burkert,[3] S.L. Careccia,[29] D.S. Carman,[3] P.L. Cole,[19] P. Collins,[5,*] V. Crede,[17] A. D'Angelo,[21,32] A. Daniel,[28] N. Dashyan,[40] R. De Vita,[20] A. Deur,[3] B. Dey,[9] S. Dhamija,[16] R. Dickson,[9] C. Djalali,[34] D. Doughty,[12,3] M. Dugger,[5] R. Dupre,[4] A. El Alaoui,[4] P. Eugenio,[17] S. Fegan,[37] T.A. Forest,[19] M.Y. Gabrielyan,[16] G. Gavalian,[29] G.P. Gilfoyle,[31] K.L. Giovanetti,[2] F.X. Girod,[11,†] J.T. Goetz,[6] W. Gohn,[13] R.W. Gothe,[34] K.A. Griffioen,[39] M. Guidal,[22] N. Guler,[29] L. Guo,[3,‡] H. Hakobyan,[36,40] C. Hanretty,[17] N. Hassall,[37] M. Holtrop,[26] Y. Ilieva,[34,18] D.G. Ireland,[37] B.S. Ishkhanov,[33] S.S. Jawalkar,[39] H.S. Jo,[22] D. Keller,[28] M. Khandaker,[27] P. Khetarpal,[30] W. Kim,[24] F.J. Klein,[10] V. Kubarovsky,[3,30] S.V. Kuleshov,[36,23] V. Kuznetsov,[24] K. Livingston,[37] M. Mayer,[29] M.E. McCracken,[9] B. McKinnon,[37] C.A. Meyer,[9] K. Mikhailov,[23] T. Mineeva,[13] V. Mokeev,[33,3] B. Moreno,[11] K. Moriya,[9] B. Morrison,[5] H. Moutarde,[11] E. Munevar,[18] P. Nadel-Turonski,[10,†] S. Niccolai,[22] M. Osipenko,[20] A.I. Ostrovidov,[17] S. Park,[17] E. Pasyuk,[5] Y. Perrin,[25] S. Pisano,[22] O. Pogorelko,[23] S. Pozdniakov,[23] J.W. Price,[7] S. Procureur,[11] Y. Prok,[38,§] D. Protopopescu,[37] B.A. Raue,[16,3] G. Ricco,[20] M. Ripani,[20] B.G. Ritchie,[5] G. Rosner,[37] F. Sabatié,[11] M.S. Saini,[17] J. Salamanca,[19] C. Salgado,[27] R.A. Schumacher,[9] E. Seder,[13] H. Seraydaryan,[29] Y.G. Sharabian,[3] D.I. Sober,[10] D. Sokhan,[14] S.S. Stepanyan,[24] P. Stoler,[30] I.I. Strakovsky,[18] S. Strauch,[34,18] D.J. Tedeschi,[34] S. Tkachenko,[29] B. Vernarsky,[9] M.F. Vineyard,[35] E. Voutier,[25] D.P. Watts,[37,¶] D.P. Weygand,[3] M.H. Wood,[8,34] L. Zana,[26] J. Zhang,[29] and B. Zhao[13,**]

(The CLAS Collaboration)

[1] *INFN, Laboratori Nazionali di Frascati, 00044 Frascati, Italy*
[2] *James Madison University, Harrisonburg, Virginia 22807*
[3] *Thomas Jefferson National Accelerator Facility, Newport News, Virginia 23606*
[4] *Argonne National Laboratory, Argonne, Illinois 60441*
[5] *Arizona State University, Tempe, Arizona 85287-1504*
[6] *University of California at Los Angeles, Los Angeles, California 90095-1547*
[7] *California State University, Dominguez Hills, Carson, CA 90747*
[8] *Canisius College, Buffalo, NY*
[9] *Carnegie Mellon University, Pittsburgh, Pennsylvania 15213*
[10] *Catholic University of America, Washington, D.C. 20064*
[11] *CEA, Centre de Saclay, Irfu/Service de Physique Nucléaire, 91191 Gif-sur-Yvette, France*
[12] *Christopher Newport University, Newport News, Virginia 23606*
[13] *University of Connecticut, Storrs, Connecticut 06269*
[14] *Edinburgh University, Edinburgh EH9 3JZ, United Kingdom*
[15] *Fairfield University, Fairfield CT 06824*
[16] *Florida International University, Miami, Florida 33199*
[17] *Florida State University, Tallahassee, Florida 32306*
[18] *The George Washington University, Washington, DC 20052*
[19] *Idaho State University, Pocatello, Idaho 83209*
[20] *INFN, Sezione di Genova, 16146 Genova, Italy*
[21] *INFN, Sezione di Roma Tor Vergata, 00133 Rome, Italy*
[22] *Institut de Physique Nucléaire ORSAY, Orsay, France*
[23] *Institute of Theoretical and Experimental Physics, Moscow, 117259, Russia*
[24] *Kyungpook National University, Daegu 702-701, Republic of Korea*
[25] *LPSC, Université Joseph Fourier, CNRS/IN2P3, INP, Grenoble, France*
[26] *University of New Hampshire, Durham, New Hampshire 03824-3568*
[27] *Norfolk State University, Norfolk, Virginia 23504*
[28] *Ohio University, Athens, Ohio 45701*
[29] *Old Dominion University, Norfolk, Virginia 23529*
[30] *Rensselaer Polytechnic Institute, Troy, New York 12180-3590*
[31] *University of Richmond, Richmond, Virginia 23173*
[32] *Universita' di Roma Tor Vergata, 00133 Rome Italy*
[33] *Skobeltsyn Nuclear Physics Institute, 119899 Moscow, Russia*
[34] *University of South Carolina, Columbia, South Carolina 29208*
[35] *Union College, Schenectady, NY 12308*
[36] *Universidad Técnica Federico Santa María, Casilla 110-V Valparaíso, Chile*
[37] *University of Glasgow, Glasgow G12 8QQ, United Kingdom*

[38] University of Virginia, Charlottesville, Virginia 22901
[39] College of William and Mary, Williamsburg, Virginia 23187-8795
[40] Yerevan Physics Institute, 375036 Yerevan, Armenia

(Dated: December 24, 2009)

Differential cross sections of the reaction $\gamma d \to K^+\Sigma^-(p)$ have been measured with the CLAS detector at Jefferson Lab using incident photons with energies between 1.1 and 3.6 GeV. This is the first complete set of strangeness photoproduction data on the neutron covering a broad angular range. At energies close to threshold and up to $E_\gamma \sim 1.8$ GeV, the shape of the angular distribution is suggestive of the presence of s-channel production mechanisms. For $E_\gamma > 1.8$ GeV, a clear forward peak appears and becomes more prominent as the photon energy increases, suggesting contributions from t-channel production mechanisms. These data can be used to constrain future analysis of this reaction.

PACS numbers: 25.20.Lj, 13.30.-a, 13.60.Le, 14.20.Gk, 14.40.Aq

A major goal of hadron physics is to study the structure of the nucleon and its excited states. However, understanding nucleon resonance excitation is a serious challenge due to the non-perturbative nature of QCD at low energies. This makes the situation for the excited states of the nucleon (N and Δ resonances) still unclear: many more states are predicted than observed and states with certain quantum numbers appear at energies much lower than predicted. This has been known for a long time as the "missing resonance" problem [1]. In quark models (see Ref. [2] for reviews), the number of excited states is determined by the effective degrees of freedom, while their ordering and decay properties are related to the residual quark-quark interaction.

The effective degrees of freedom in standard non-relativistic quark models are three equivalent valence quarks with one-gluon exchange interactions. A different class of models uses interactions that give rise to a quark-diquark clustering of the baryon [3]. If there is a tightly bound diquark, only two degrees of freedom are available at low energies; thus, fewer states are predicted. Furthermore, selection rules in the decay pattern may arise from the quantum numbers of a diquark. More states are provided by collective models of the baryon, like the algebraic approach [4], or in the framework of flux-tube models [5], which are motivated by lattice QCD. So far, however, the experimentally observed number of states is still far lower than predicted by the quark-diquark models.

Experimentally, most of our present knowledge of baryon resonances comes from reactions involving pions in the initial and/or final states. For increasing masses, both the energy overlap of the resonances and meson production make it more difficult to separate the resonance contributions. A possible explanation for the missing resonance problem could be that pionic coupling to the intermediate N^* or Δ^* states is weak and that many of the missing states only become visible in other reaction channels. Photoproduction of non-strange resonances detected via decay into strange particles offers two benefits: (1) two-body KY (where Y denotes any hyperon) final states are easier to analyze than the three-body $\pi\pi N$ final states that dominate the decays at higher masses resonances; (2) couplings of nucleon resonances to KY final states are expected to differ from those to πN and $\pi\pi N$ final states [6]. Therefore, looking in the strangeness sector casts a different light on the resonance excitation spectrum, and thus, may emphasize resonances not revealed in πN scattering. To date, however, the PDG compilation [7] gives poorly known $K\Lambda$ couplings for only five well-established resonances, and no $K\Sigma$ couplings for any resonances. Mapping out the spectrum of excited states that decay into KY particles is therefore crucial to provide a deeper insight into the underlying degrees of freedom of the nucleon and to discriminate among different models.

The search for missing resonances requires more than the study of the hadronic mass spectrum. In fact, QCD cannot be directly tested against experimental N^* mass spectra without a model for the production dynamics [8]. Thus, in addition to the s-channel contributions, important in the resonance region in order to reproduce the invariant mass spectra, the t- and u-channel meson and baryon exchanges are also necessary in the theoretical description. The former are needed in order to describe the diffractive part of the production, and u-channel diagrams are necessary to describe the back-angle production. Thus, measurements that can constrain the phenomenology for these reactions are just as important as finding one or more of the missing resonances.

A large amount of cross-section data of hyperon photoproduction on the proton has been published in recent years by the SAPHIR [9], CB-ELSA/TAPS [10, 11],

*Current address:Catholic University of America, Washington, D.C. 20064
†Current address:Thomas Jefferson National Accelerator Facility, Newport News, Virginia 23606
‡Current address:Los Alamos National Laboratory, Los Alamos, New Mexico 87545
§Current address:Christopher Newport University, Newport News, Virginia 23606
¶Current address:Edinburgh University, Edinburgh EH9 3JZ, United Kingdom
**Current address:College of William and Mary, Williamsburg, Virginia 23187-8795

CLAS [12, 13] and LEPS [14] collaborations from threshold up to $E_\gamma \sim 3.8$ GeV over a wide angular range. The polarization of the recoil hyperon has also been measured by CLAS [13, 15], SAPHIR [9] and GRAAL [16], while photon beam asymmetries have been measured by LEPS [17]. Despite this large body of data, theoretical ambiguities still exist. In fact, theorists have found conflicting evidence for resonances using isobar models [18], coupled-channel [19–21] and partial wave analysis [22] approaches.

In this situation the necessity of more data and from different channels is evident. In particular, for Y-photoproduction on the neutron, one can take full advantage of the isospin symmetry, adding significant constraints on the γKNY coupling constants [23]. Unfortunately, data of hyperon photoproduction on neutrons are very scarce, with the only available data from LEPS [24], covering a limited photon energy range at very forward kaon angles.

In this paper high-precision cross sections of the reaction $\gamma d \to K^+\Sigma^-(p)$ in a broad kinematic range are presented. The data were acquired using the CLAS detector [25] housed in Hall B at Jefferson Lab during a two-month period in early 2004. A bremsstrahlung photon beam produced by a 3.776 GeV continuous electron beam hitting a 10^{-4} radiation-lengths gold foil was used [26]. Tagged photons, in the energy range from 0.8 to 3.6 GeV, were directed onto a liquid-deuterium target. With an electron beam current of ~ 25 nA, the photon flux incident on the deuterium target was $\sim 10^8$ γ/s.

The CLAS detector utilized a non-uniform toroidal magnetic field generated by six superconducting coils that defines six independent sectors. The detector is instrumented with three sets of multi-wire drift chambers (DC) for charged track reconstruction. Two layers of scintillator counters (TOF) and lead-scintillator electromagnetic calorimeters (EC) provide charged-particle time-of-flight measurements and neutral particle measurement, respectively.

The torus field polarity was such that positive particles were bent out of the beam line. The data under analysis in this work was acquired with roughly equal numbers of triggers at torus settings of 2250 A (60% of full field) and 3375 A (90% of full field). The first has better acceptance at forward angles, especially for negatively charged particles, while the second has better momentum resolution. The integrated luminosity collected during the entire run period was about 50 pb^{-1}, equally divided between the two torus-field settings. The analysis procedure described below has been applied separately to the low and high torus-field data. The cross sections from each data set were then combined to obtain the final results.

The primary kaon, and the pion and neutron coming from the Σ^- decay (with branching fraction $b_{\Sigma^-} \sim 100)\%$ were detected by CLAS. The low-energy spectator proton was reconstructed using the missing-mass technique. The energy and momentum of each charged particle were corrected for the mean energy lost prior to reaching the DC and for misalignments of the tracking system. Fiducial cuts were applied to both real and Monte-Carlo simulated data in order to exclude regions where the detector acceptance was not well understood (*e.g.* extreme forward or backward angles, and near the torus coils) and the regions where the DC or scintillator efficiencies were not well known.

Special care was devoted to the kaon identification because of the large background due to out-of-time protons and pions that contaminate the kaon sample. The difference at the interaction point between the initial photon time, measured by the tagging system, and the kaon production time, measured by the TOF system, was used to identify the good kaons. The distribution of this vertex-time difference peaks at zero for good kaons. The out-of-time particles were removed by a 3σ cut around the peak. In addition, the reconstructed kaon reaction vertex was required to be located within the target.

Neutral particles are identified in CLAS as clusters in the EC that are not associated with any charged track in the DC. Neutral clusters with $\beta > 0.9$ are then identified as photons, while clusters with $\beta < 0.9$ are associated with neutrons. The CLAS calorimeters are usually calibrated using $\beta = 1$ particles; thus, the identification of slower neutrons required the development of a set of dedicated routines in order to obtain their correct time of flight and to calculate their β. These corrections were tested and validated by analyzing $\gamma d \to p\pi^+\pi^- n$ events and comparing the reconstructed 4-momentum of the neutron with the missing 4-momentum of the three charged particles. In addition, the detached Σ^- decay vertex was also taken into account when calculating the neutron path.

Events passing the above selection criteria were labeled as $\gamma d \to K^+\pi^- nX$ candidates. To identify events consistent with the missing particle X as a spectator proton, we first applied a cut on the missing momentum $P_X \leq 0.25$ GeV/c. The remaining events, integrated over all angles, were divided into 100 MeV wide bins in photon energy. In each bin, the missing-mass distribution was used to select events consistent with a missing spectator proton.

The missing-mass distribution for the photon energy bin of 2.0–2.1 GeV in Fig. 1 shows a clear proton peak and a smaller structure at higher masses. The latter, that starts to appear at photon energies $\gtrsim 2$ GeV, is due to photoproduction events of $\Sigma^*(1385)^-$ and $K^*(892)^+$. The $\Sigma^*(1385)^-$ decays into $\Sigma\pi$ with $b_{\Sigma^*} \sim 12\%$ and the $K^*(892)^+$ decays into $K\pi$ with $b_{K^*} \sim 100\%$. Each missing-mass distribution was fit with two Gaussian line shapes plus a polynomial curve. Events with a spectator proton were selected by applying a 3σ cut around the main peak. The background contribution coming from $\Sigma^*(1385)^-$ and $K^*(892)^+$ events was estimated to be between 1 and 3% and then subtracted.

After the selection of $\gamma d \to K^+\pi^- n(p)$ candidates, we looked for evidence of the presence of Σ^- particles in the invariant-mass distribution of the pion and neutron.

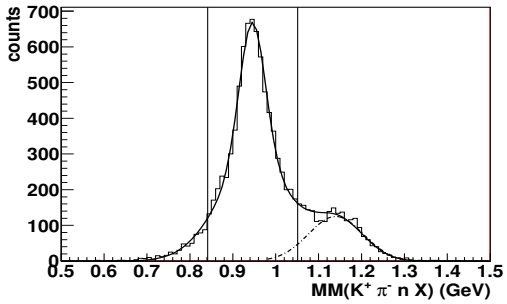

FIG. 1: Missing-mass distribution of the $\gamma d \to K^+\pi^- nX$ reaction for the low torus-field data and photon energy in the bin 2.0–2.1 GeV. The solid line is the total fit to the distribution, while the dot-dashed line is the contribution of the events with an additional π^0 as explained in the text. The two vertical lines represent a 3σ cut.

The distribution obtained for the low torus-field data and the photon-energy bin 2.0–2.1 GeV is shown in Fig. 2. A sharp peak consistent with the Σ^- appears on top of a small, almost flat background. Each distribution was fitted with a Lorentzian peak plus a second-order polynomial for the background. The final sample of $\gamma d \to K^+\Sigma^-(p)$ events was obtained by selecting events within 3Γ around the peak, where Γ is the full width at half maximum of the Lorentzian. The background calculated by integrating the polynomial curve within the cuts was subtracted. The total background is generally increasing with the photon energy, and is between 5% and 25% for the low torus-field data and between 2% and 15% for the high torus-field data.

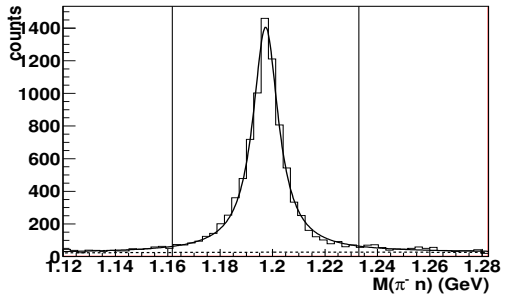

FIG. 2: The $n\pi^-$ invariant mass distribution for the low torus-field data in the photon energy range 2.0–2.1 GeV. The solid line is the fit of the distribution with a Lorentzian peak plus a polynomial background (the latter represented by the dashed line). The two vertical lines show the 3Γ cut applied to the data sample in order to select Σ^- events.

Finally, the extracted yield was corrected for the CLAS detector acceptance. For this, $\gamma d \to K^+\Sigma^- p$ events were generated according to the Quark-Gluon Strings Model [27, 28]. The Fermi motion of the neutron bound in the deuterium nucleus was described by the momentum distribution calculated from the Paris potential [29]. The generated events were processed through a GEANT-based Monte Carlo simulation of the CLAS detector, incorporating all of the known subsystem efficiencies and resolutions. The simulated data were analyzed by the same software used in the real data processing and analysis. The CLAS acceptance was computed as the ratio between the number of events passing all the analysis cuts and the number of generated events in each one of the 100-MeV wide photon energy bins and 0.1-wide $\cos\theta_K^{\rm c.m.}$ bins.

The differential cross section for $K^+\Sigma^-$ photoproduction on the neutron was calculated using the following relation:

$$\frac{d\sigma}{d\Omega} = \frac{A}{\rho x N_A}\frac{N^W_{peak} b_{\Sigma^-}}{N_\gamma\,\Delta\Omega}\,(1-B)\,, \qquad (1)$$

where N^W_{peak} is the number of the $\gamma d \to K^+\Sigma^-(p)$ events weighted by the acceptance of the CLAS detector, N_γ is the number of incident photons, B is the fraction of background events, A is the target molecular weight, N_A is Avogadro's number, and $\rho = 0.163$ g/cm^3 and $x = 24$ cm are the target density and length, respectively. The number of incident photons was calculated using the tagging efficiency, measured during dedicated low-intensity ($\sim 10^5$ γ/s) runs using a 100% efficient lead-glass total absorption counter, and the number of out-of-time electrons detected in the tagging system during normal data taking runs [30]. Photon absorption in the target was also calculated and found to be negligible. Cross sections from the low and high torus-field data were weight averaged.

Systematic uncertainties of the final cross sections contain contributions from the photon flux calculation (4%), target length and density (0.5%), fiducial cuts (1–3%, depending on the bin), background subtraction (1–10%), neutron detection efficiency (0.7%) and the Monte Carlo event generator (1.7%). The total systematic uncertainty was obtained by adding in quadrature each contribution, bin by bin. Thus, the total systematic uncertainty in our cross section measurements is estimated to be about 4.5–13.5%.

Our final results are shown as full circles in Fig. 3. The error bars (upper bands) represent the statistical (systematic) uncertainties. This is the first high-precision determination of Σ^- photoproduction on the neutron covering a broad kaon-angle and photon-energy range. At a photon energy of ~ 1.8 GeV, a clear forward peak starts to appear and becomes more prominent as the photon energy increases. This behavior, that is typically attributed to contributions from t-channel mechanisms, is not observed at lower energies, where the dominant contributions appear to be from s-channel mechanisms. Above $\sim$2.0 GeV, there are indications of a possible backward peak, which might suggest the presence of u-channel mechanisms.

The few LEPS data [24] available for energies 1.5–2.4 GeV and at forward angles are shown in Fig. 3. Since these data have been provided in 50-MeV wide energy bins, for comparison with our results the weighted average of two bins has been computed and reported in the

figure. They are in good agreement with our results within the total uncertainties.

Also shown in Fig. 3 are the theoretical results of a Regge-based calculation (Regge-3 model) [31]. In this model, the reaction amplitude incorporates the exchange of K^+ and $K^*(892)^+$ Regge trajectories. By adding resonance contributions to the Regge amplitudes, the model is able to describe the Λ and Σ^0 photo- and electroproduction data on the proton reasonably well [32–34]. The model, however, overestimates the magnitude of our data on the neutron (although, the angular distribution predicted by the model is qualitatively similar to the measured one). We note here that for the neutron calculation no resonances were included in the predictions, having only the background contribution.

In conclusion, CLAS has provided the first precise determination of the $\gamma d \to K^+\Sigma^-(p)$ cross section in a broad kinematic range where almost no γn data are available. These results will significantly contribute to the improvement of the phenomenological analysis of meson photoproduction reactions at medium energies aiming to solve the missing resonance problem.

We would like to acknowledge the outstanding efforts of the staff of the Accelerator and the Physics Divisions at JLab that made this experiment possible. This work was supported in part by the Italian Istituto Nazionale di Fisica Nucleare, the French Centre National de la Recherche Scientifique and the Commissariat à l'Energie Atomique, the U.S. Department of Energy and the National Science Foundation, the National Research Foundation of Korea, and the UK Science and Technology Facilities Council (STFC). The Southeastern Universities Research Association (SURA) operated the Thomas Jefferson National Accelerator Facility for the United States Department of Energy under contract DE-AC05-84ER40150 during this work.

[1] N. Isgur and G. Karl, Phys. Rev. D **18**, 4187 (1978); Phys. Rev. D **19**, 2653 (1979) and Phys. Rev. D **20**, 1191 (1979).
[2] S. Capstick and W. Roberts, Prog. Part. Nucl. Phys. **45**, 241 (2000); A. J. G. Hey and R. L. Kelly, Phys. Reports **96**, 71 (1983).
[3] M. Anselmino *et al.*, Rev. Mod. Phys. **65**, 1199 (1993).
[4] R. Bijker *et al.*, Ann. of Phys. **236**, 69 (1994).
[5] N. Isgur and J. Paton, Phys. Rev. D **31**, 2910 (1985).
[6] S. Capstick and W. Roberts, Phys. Rev. D **49**, 4570 (1994); Phys. Rev. D **57**, 4301 (1998) and Phys. Rev. D **58**, 74011 (1998).
[7] C. Amsler *et al.* (Particle Data Group), Phys. Lett. B **667**, 1 (2008).
[8] T. S. H. Lee and T. Sato, Proceedings of the N^*2000 Conference, eds. Burkert *et al.*, (World Scientific, Singapore, 2001), p.215 and Phys. Rev. C **66**, 055212 (2002).
[9] K. -H. Glander *et al.*, Eur. Phys. J. A **19**, 251 (2004).
[10] R. Castelijins *et al.*, Eur. Phys. J. A **35**, 39 (2008).
[11] M. Nanova *et al.*, Eur. Phys. J. A **35**, 333 (2008).
[12] R. Bradford *et al.*, Phys. Rev.C **73**, 035202 (2006).
[13] M. McCracken, Ph.D. thesis 2008, Carnegie Mellon University, web:http://www.jlab.org/Hall-B/general/clas_thesis.html, and arXiv:0912.4274v2 [nucl-ex], to be published.
[14] M. Sumihama *et al.*, Phys. Rev. C **73**, 035214 (2006).
[15] J. W. C. McNabb *et al.*, Phys. Rev. C**69**, 035202 (2006).
[16] A. Lleres *et al.*, Eur. Phys. J. A **31**, 79 (2007).
[17] H. Kohri *et al.*, Phys. Rev. Lett. **97**, 082003 (2006).
[18] T. Mart and C. Bennhold, Phys. Rev. C **61**, 012201 (1999).
[19] V. Shklyar, H. Lenske and U. Mosel, Phys. Rev. C **72**, 015210 (2005).
[20] A. V. Anisovich *et al.*, Eur. Phys. J. A **34**, 243 (2007).
[21] B. Julia-Diaz *et al.*, Nucl. Phys. A **755**, 463 (2005).
[22] A. V. Sarantsev *et al.*, Eur. Phys. J. A **25**, 441 (2005).
[23] T. Mart, C. Bennhold and C.E.Hyde-Wright, Phys. Rev. C **51**, 1074(R) (1995).
[24] H. Kohri *et al.*, Phys. Rev. Lett. **97**, 082003 (2006).
[25] B. A. Mecking *et al.*, Nucl. Instrum. Methods A **503**, 444 (2003).
[26] D. I. Sober *et al.*, Nucl. Instrum. Methods A **440**, 263 (2000).
[27] V. Yu. Grishina *et al.*, Eur. Phys. J. A **10**, 355 (2001); Eur. Phys. J. A **19**, 117 (2004) and Eur. Phys. J. A **25**, 141 (2005).
[28] V. Yu. Grishina and L. Kondratiuk, Private Communication.
[29] M. Lacombe *et al.*, Phys. Rev. C **21**, 861 (1980).
[30] J. Ball and E. Pasyuk, Photon Flux Determination Through Sampling of "outoftime" Hits with the Hall B Photon Tagger, web:http://www1.jlab.org/ul/Physics/Hall-B/clas/public/2005002.pdf
[31] P. Vancraeyveld, L. De Cruz, J. Ryckebusch and T. Van Cauteren, Phys. Lett. B**681**, 428 (2009).
[32] T. Corthals, J. Ryckebusch and T. Van Cauteren, Phys. Rev. C **73**, 045207 (2006).
[33] T. Corthals, D. G. Ireland, T. Van Cauteren and J. Ryckebusch, Phys. Rev. C **75**, 045204 (2007).
[34] T. Corthals, T. Van Cauteren, P. Vancraeyveld, J. Ryckebusch and D. G. Ireland, Phys. Lett. B **656**, 186 (2007).

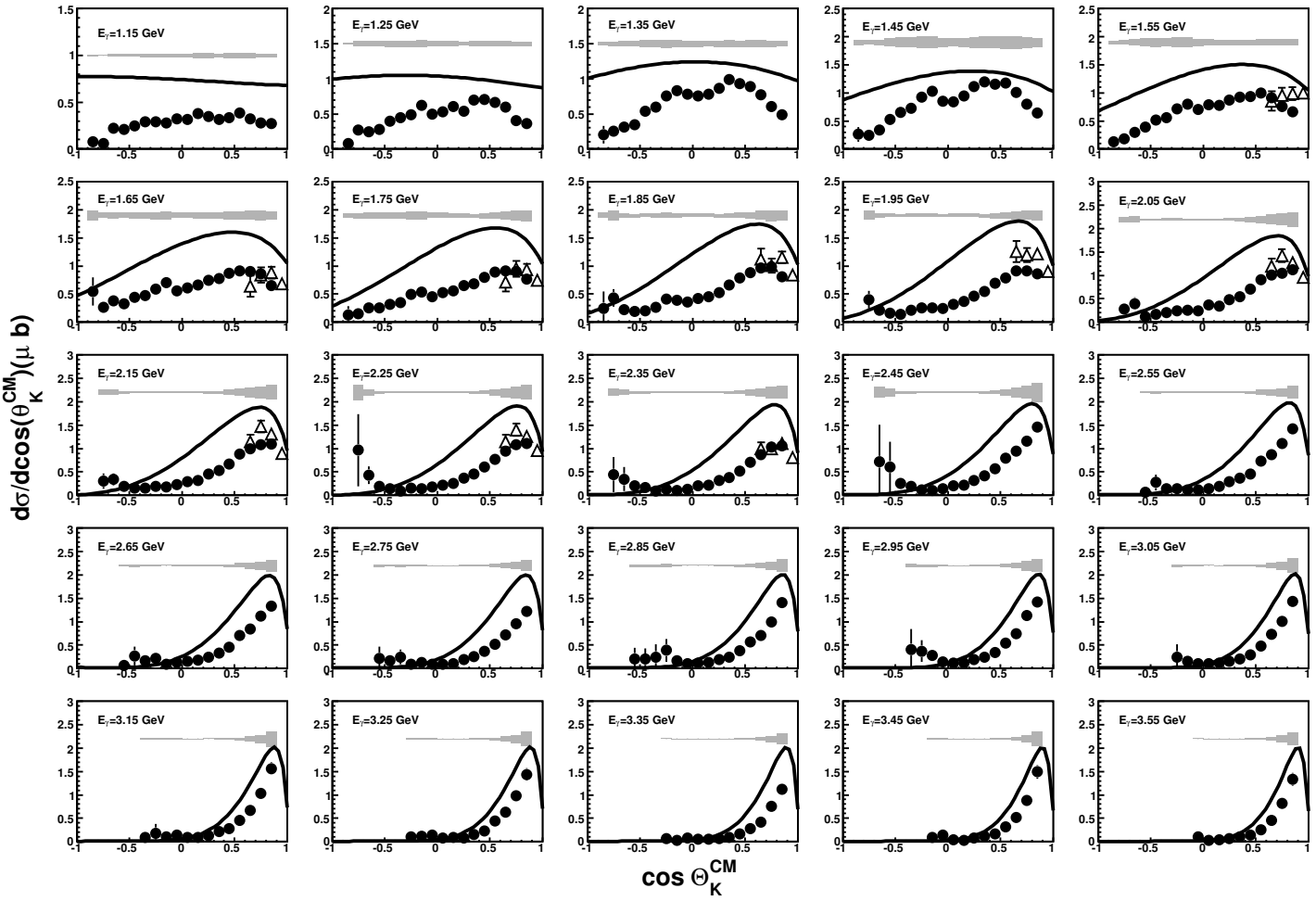

FIG. 3: Differential cross sections of the reaction $\gamma d \to K^+\Sigma^-(p)$ obtained by CLAS (full circles). The error bars represent the statistical uncertainty and the bands on top the systematic uncertainty. LEPS data [24] (empty triangles) and a Regge-3 model prediction [31] (solid curve) are also shown.